Biosensors and Bioelectronics 42 (2013) 207–213

Contents lists available at SciVerse ScienceDirect

Biosensors and Bioelectronics

journal homepage: www.elsevier.com/locate/bios

Direct electrochemistry of hemoglobin on graphene and titanium dioxide nanorods composite modified electrode and its electrocatalysis

Wei Sun [a,b,*], Yaqing Guo [b], Xiaomei Ju [b], Yuanyuan Zhang [b], Xiuzhen Wang [b], Zhenfan Sun [a]

[a] College of Chemistry and Chemical Engineering, Hainan Normal University, 53 Zhenzhou Road, Haikou 571158, PR China
[b] College of Chemistry and Molecular Engineering, Qingdao University of Science and Technology, Qingdao 266042, PR China

ARTICLE INFO

Article history:
Received 27 July 2012
Received in revised form
21 September 2012
Accepted 8 October 2012
Available online 17 October 2012

Keywords:
Graphene
Titanium dioxide nanorods
Hemoglobin
Direct electrochemistry
Electrocatalysis

ABSTRACT

A biocompatible sensing platform based on graphene (GR) and titanium dioxide (TiO_2) nanorods for the immobilization of hemoglobin (Hb) was adopted in this paper. The GR–TiO_2–Hb composite-modified carbon ionic liquid electrode was constructed through a simple casting method with Nafion as the film forming material. UV–Vis and FT–IR spectra confirmed that Hb retained its native structure in the composite film. Direct electron transfer of Hb incorporated into the composite was realized with a pair of quasi-reversible redox waves appeared, indicating that the presence of GR–TiO_2 nanocomposite on the electrode surface could facilitate the electron transfer rate between the electroactive center of Hb and the substrate electrode. Hb modified electrode showed excellent electrocatalytic activity to the reduction of trichloroacetic acid in the concentration range from 0.6 to 21.0 mmol L^{-1}. These results indicated that GR–TiO_2 nanocomposite could be a friendly biocompatible interface for immobilizing biomolecules and keeping their native structure. The fabricated biosensor displayed the advantages such as high sensitivity, good reproducibility and long-term stability.

1. Introduction

Researches on direct electrochemistry of redox proteins have aroused increasing interests, which not only help to elucidate the intrinsic thermodynamic and kinetic properties of proteins, but also apply to fabricate bioelectronic devices (Armstrong et al., 1988; Leger et al., 2003). Also direct electron transfer between redox proteins and electrode can establish a model for the mechanism study on the electron exchange among enzymes in biological systems, and provide basis for fabricating electrochemical biosensors and catalytic bioreactors without mediators (Armstrong and Wilson, 2000). In general, direct electrochemistry of redox proteins on the conventional electrodes is difficult to be realized due to the deeply buried redox active center in the proteins or the unfavorable orientations of protein on the electrode surface. Therefore, great efforts have been developed to construct a matrix to enhance the electron transfer rate between the electrode and redox protein.

Recently graphene (GR) has become the hot research topics in different fields because of many intriguing attributes it displays (Geim and Novoselov, 2007; Guo and Dong, 2011). GR is a single layer of carbon atoms with a hexagonal arrangement in a two-dimensional lattice, which can be regarded as the basic building block for the related graphitic materials. GR exhibits high surface area and excellent electrical conductivity, and the increase of effective surface area helps to introduce a large number of active sites (Zhu et al., 2010). Other unique properties of GR include fast electron transportation, high thermal conductivity, excellent mechanical stiffness and good biocompatibility (Chen et al., 2008, 2010), which result in many applications including supercapacitors, batteries and electromechanical resonators. Electrochemistry and electroanalysis of GR had been reviewed by different research groups with its potentials applications described (Shao et al., 2010; Gan and Hu, 2011). Wang et al. (2009b) adopted the GR-modified electrode to selectively detect dopamine in a large excess of ascorbic acid. Li et al. (2009) fabricated a GR and Nafion based electrochemical platform for ultrasensitive detecting of cadmium ion. Wu et al. (2010) utilized chitosan-dispersed GR to immobilize cytochrome C for the electrocatalytic determination of nitric oxide. Xu et al. (2010) utilized chitosan-GR composite film for encapsulation of Hb to detect hydrogen peroxide. Deng et al. (2013) applied an electrochemically reduced graphene oxide modified glassy carbon electrode (GCE) for the detection of L-tryptophan and L-tyrosine.

As a semiconductive material, TiO_2 is widely used in cosmetics, solar cells, batteries, additives in toothpaste and white paint. Recently, there are considerable interests in using TiO_2 nanoparticles due to the properties such as high surface area, optical transparency

* Corresponding author. Tel./fax: +86 898 31381637.
E-mail address: swyy26@hotmail.com (W. Sun).

0956-5663/$ - see front matter © 2012 Elsevier B.V. All rights reserved.
http://dx.doi.org/10.1016/j.bios.2012.10.034

and good biocompatibility. Various TiO_2 nanoparticles have been used to immobilize proteins or enzymes on electrode surface for either mechanistic study or fabricating electrochemical biosensors. Topoglidis et al. (2000, 2001) immobilized different proteins into nanoporous TiO_2 film electrodes as the electrochemical or optical biosensors. Li et al. (2001) applied nanocrystalline TiO_2 films on electrodes to entrap heme proteins and observed their direct electrochemistry. Bao et al. (2008) fabricated uniformly porous nanostructured TiO_2 materials for direct electrochemistry of glucose oxidase and glucose sensing. Sun et al. (2009b) investigated the direct electrochemistry of hemoglobin (Hb) on a chitosan and TiO_2 nanoparticle composite modified electrode and its electrocatalysis. Zhang et al. (2004) fabricated a hydrogen peroxide biosensor with horseradish peroxidase and TiO_2 nanoparticle modified electrode. So TiO_2 nanomaterials have been widely used in the fields of electroanalysis and electrochemical biosensors.

Nafion is a proton-conductive and biocompatible perfluorosulfonate linear polymer, which exhibits excellent film-forming ability and has been widely used for the immobilization of enzymes (Lu et al., 2007; Nadzhafova et al., 2004). The presence of Nafion can form a stable film to enhance the stability of protein immobilized on the electrode surface and prevent the leakage of protein from electrode into the solution. Carbon ionic liquid electrode (CILE), which is prepared by using ionic liquid (IL) as the binder and the modifier in carbon paste electrode, has been widely used in recent years. CILE has been proven to have the advantages such as easy preparation, high electrochemical stability, good ionic conductivity and wide electrochemical windows (Opallo and Lesniewski, 2011). Shangguan et al. (2008) applied CILE in the electrochemical detection of paracetamol. Zhang and Zheng (2007) investigated the electrochemical behavior of hydroquinone on CILE. Our group also applied CILE to the investigation on electrochemistry of protein and electroactive molecules (Sun et al., 2008, 2009a).

In this paper, a GR–TiO_2 nanocomposite was prepared and used for the investigation of the electrochemistry of Hb. GR based composites have aroused great attentions due to the synergistic properties originated from the individual components and their interaction (Singh et al., 2011). Zou et al. (2011) synthesized a GR–TiO_2 nanocomposite by refluxing mixing solutions of graphene oxide with peroxotitanium complexes and investigated their photoelectrical properties. Wang et al. (2009a) prepared a self-assembled TiO_2–GR hybrid nanostructure with enhanced Li-ion insertion/extraction properties. Zhang et al. (2010) applied GR–TiO_2 nanocomposite as the photocatalysis for the photodegradation of methylene blue with significant enhanced reaction rate. Sun et al. (2011) combined chitosan–IL–TiO_2–GR nanocomposite film-modified electrode for the investigation on electrochemistry of Hb. Jang et al. (2012) fabricated a glucose biosensor based on TiO_2–GR composite-modified GCE. The results indicated that GR–TiO_2 nanocomposite could exhibit specific photophysical and electrochemical properties, which had the potential applications for the electrochemical sensing. In this work, GR–TiO_2 nanocomposite was cast on the surface of CILE and further used for the immobilization of Hb. Direct electron transfer between Hb and CILE was further investigated by cyclic voltammetry. The composite film could retain the bioactivity of Hb and provide a favorable microenvironment for Hb to exchange the electrons. The Hb modified electrode exhibited good electrocatalysis to trichloroacetic acid. Therefore GR–TiO_2 composite film could be used as the biomaterial suitable for protein immobilization and biosensors preparation.

2. Experimental

2.1. Reagents

Bovine hemoglobin (Hb, MW. 64500, Sinopharm Chemical Reagent Ltd. Co., China), 1-butylpyridinium hexafluorophosphate ($BPPF_6$, Lanzhou Greenchem ILS. LICP. CAS., China), graphite powder (particle size 30 μm, Shanghai Colloid Chem. Co., China), Nafion (5%, Sigma, USA) and trichloroacetic acid (TCA, Tianjin Kemiou Chemical Ltd. Co., China) were used as received. Graphene (GR) was synthesized according to previous reports (Hummers and Offeman, 1958) and TiO_2 nanorods were synthesized according the reported method with minor modification (Wu et al., 2006). 0.2 mol L^{-1} phosphate buffer solutions (PBS) with various pH values were used as the supporting electrolyte. All the other chemicals used were of analytical reagent grade and doubly distilled water was used in the experiments.

2.2. Apparatus

All the electrochemical measurements were executed on a CHI 750B electrochemical workstation (Shanghai CH Instrument, China). A conventional three-electrode system was used with a Hb modified electrode as working electrode, a platinum wire as auxiliary electrode and a saturated calomel electrode (SCE) as reference electrode. UV–Vis is absorption spectra and FT–IR spectra were recorded on a Cary 50 probe spectrophotometer (Varian Company, Australia) and Tensor 27 FT–IR spectrophotometer (Bruker Company, Germany). Scanning electron microscopy (SEM) was recorded on a JSM-6700 F scanning electron microscope (Japan Electron Company, Japan).

2.3. Procedure

CILE was fabricated according to a reported procedure (Sun et al., 2008). 3.0 g graphite powder and 1.0 g $BPPF_6$ were mixed thoroughly in an agate mortar. The homogeneous paste was packed into a cavity of a glass tube (Φ=4 mm) and a copper wire was inserted through the opposite end to establish an electrical contact. Prior to use the electrode was polished on a weighing paper to get a mirror-like surface.

The nanocomposite was prepared by mixing 60 μL of 2.0 mg mL^{-1} GR suspension solution, 100 μL of 2.0 mg mL^{-1} TiO_2 nanorods suspension solution and 120 μL of 30 mg mL^{-1} of Hb solution homogeneously. Then 8 μL of the mixture was cast on CILE surface and left to dry at room temperature. This resulted electrode was denoted as GR–TiO_2–Hb/CILE. Finally, 5 μL of 0.5% Nafion solution was spread evenly onto the surface of GR–TiO_2–Hb/CILE to get Nafion/GR–TiO_2–Hb/CILE. Other modified electrodes including Nafion/GR–Hb/CILE, Nafion/TiO_2–Hb/CILE, Nafion/Hb/CILE were prepared by the similar procedure and used for comparison.

3. Results and discussion

3.1. Scanning electron microscopic images

The surface morphologies of GR, TiO_2 nanorods and their hybrid films were examined by SEM. As shown in Fig. 1a, TiO_2 exhibited as nanorods with the average width of 150 nm. The SEM image of GR showed clearly large sheet-like shape with slightly scrolled edges, which was the typical result of GR nanosheets. Most GR nanosheets were lying flat with some fold together (Fig. 1b). Fig. 1c was that of GR–TiO_2 nanocomposite, which exhibited that TiO_2 nanorods were dispersed on GR surface and inserted into the layer structure of GR. The good connection between TiO_2 nanorods and GR provided a porous microstructure for the loading of proteins. As for the GR–TiO_2–Hb composite (Fig. 1d), it can be seen that Hb was embedded into GR–TiO_2 nanocomposite with the increase of surface roughness, indicating

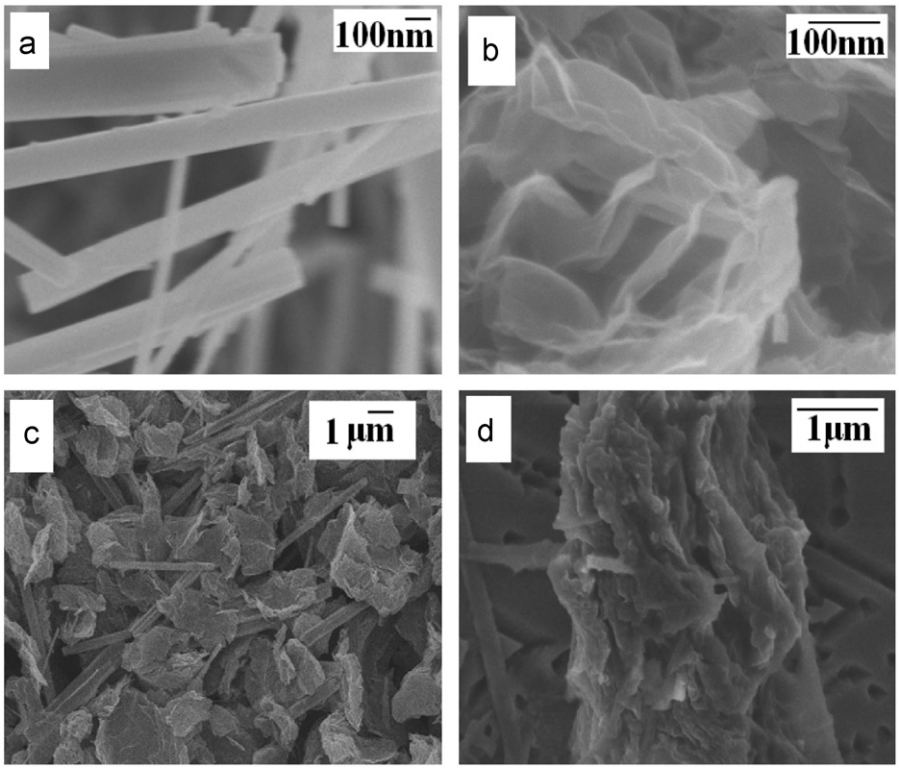

Fig. 1. SEM images of (a) TiO_2 nanorods, (b) GR, (c) GR–TiO_2 nanocomposite and (d) GR–TiO_2–Hb composite.

that Hb had been intercalated into the layered structure of GR–TiO_2 nanocomposite.

3.2. Spectroscopic results

FT–IR spectroscopy has been employed to check the conformational integrity of the heme proteins, which is very sensitive to the conformational changes of the protein (Byler and Susi, 1986). The shapes of amide I and II infrared absorption band of Hb can provide detailed information about the secondary structure of the polypeptide chain (Kauppinen et al. 1981; Rusling and Kumosinski, 1992). The amide I band (1700–1600 cm^{-1}) is caused by C=O stretching vibrations of peptide linkages in the protein's backbone and the amide II band (1600–1500 cm^{-1}) is attributed to the combination of N–H bending and C–N stretching. The amide I and II bands of Hb in GR–TiO_2 films appeared at 1649.28 and 1533.97 cm^{-1} (Fig. 2Ab), which had almost the same position with the native state of Hb at 1653.37 and 1535.73 cm^{-1} (Fig. 2Aa). UV–Vis adsorption spectroscopy is also an effective method to probe the structure change of heme proteins. The location of the Soret absorption band from the four iron heme groups of proteins provide structural information about possible denaturation of heme proteins, especially the possible denaturation or the conformational change in the heme group region (Rusling and Nassar, 1993; Zhu et al., 2002). As shown in Fig. 2B, the Hb molecules had a characteristic Soret absorption at 406.0 nm (curve a). While in mixture solutions of GR–Hb, GR–TiO_2–Hb and TiO_2–Hb (curves b–d), the Soret band also appeared at 406.0 without changes, which indicated that Hb molecules kept its native structure in the mixture. The results proved the biocompatibility of GR and TiO_2 with the protein. GR exhibit good biocompatibility with promising applications in electrochemical sensors (Chen et al., 2008). TiO_2 nanorods show good biocompatibility, stability and environmental safety, then it is used for the immobilization of heme protein (Zheng et al., 2008). These results suggested that Hb retained the essential features of its native structure without any changes after immobilized in GR–TiO_2 composite films.

3.3. Electrochemical characterization of Nafion/GR–TiO_2–Hb/CILE

Cyclic voltammograms of different electrodes were recorded in a 1.0 mmol L^{-1} $[Fe(CN)_6]^{3-/4-}$ and 0.1 mol L^{-1} KCl mixture solution with the results shown in Fig. 3A. A pair of well-defined quasi-reversible redox peaks were observed on Nafion/Hb/CILE (curve a). On Nafion/TiO_2–Hb/CILE (curve b) the electrochemical response was enhanced with the increase of the redox peak currents, indicating the addition of TiO_2 nanorods in the composite film was benefit to improve the electrochemical responses. The results can be attributed to the increase of the surface area due to the presence of semiconductive TiO_2 nanorods. On Nafion/GR–Hb/CILE (curve c), the redox peak currents also increased, which was attributed to presence of GR in the composite film. GR has the unique properties such as high specific surface area, large surface-to-volume ratio, excellent electrical conductivity and electron mobility. So the redox peak currents were greatly enhanced on the electrode surface. On Nafion/GR–TiO_2–Hb/CILE (curve d), the redox peak currents were further increased greatly, which could be attributed to the synergistic effects of GR and TiO_2 nanorods in the composite film that promoted the electron transfer rate of the redox probe.

Electrochemical impedance spectroscopy (EIS) can provide impedance information of the electrode surface during the modification process. The semicircle portion observed at high frequencies in the Nyquist diagrams corresponds to the electron transfer limiting process. As can be seen from Fig. 3B, the electron transfer resistance (Ret) of Nafion/Hb/CILE was found to be 59.1 Ω (curve a). While the Ret values of Nafion/TiO_2–Hb/CILE (curve b) and Nafion/GR–Hb/CILE (curve c) were estimated as 37.5 and 32.5 Ω, respectively, which were smaller than that of Nafion/Hb/

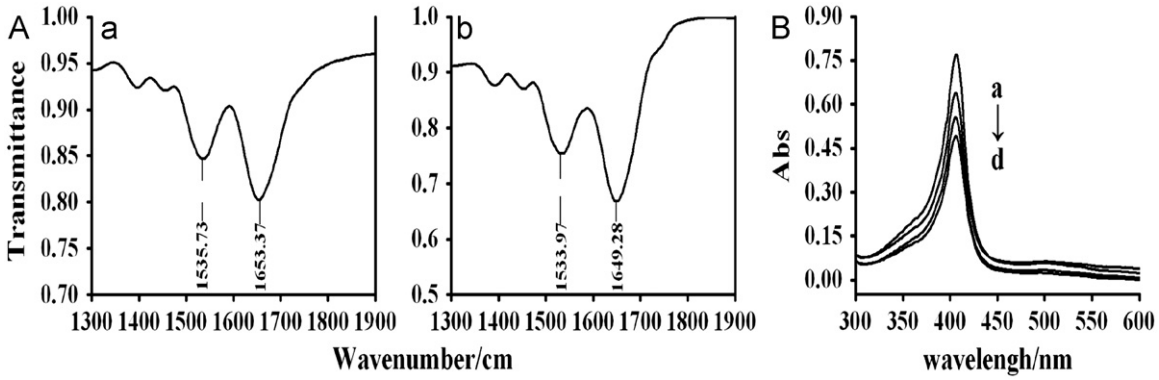

Fig. 2. (A) FT–IR spectra of (a) Hb and (b) GR–TiO_2–Hb composite, (B) UV–V is absorption spectra of (a) Hb, (b) GR–Hb, (c) GR–TiO_2–Hb, (d) TiO_2–Hb in pH 7.0 PBS.

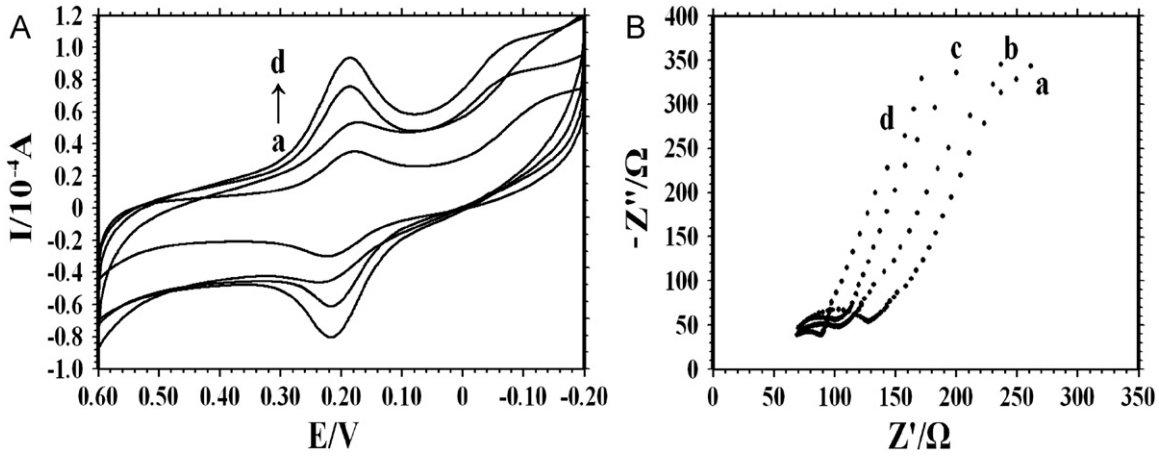

Fig. 3. (A) Cyclic voltammograms of different electrodes in a 10.0 mmol L^{-1} $[Fe(CN)_6]^{3-/4-}$ and 0.1 mol L^{-1} KCl mixture solution with scan rate as 100 mV s^{-1}. (B) EIS of different electrodes in a 5.0 mmol L^{-1} $[Fe(CN)_6]^{3-/4-}$ and 0.1 mol L^{-1} KCl mixture solution with the frequencies ranging from 10^5 to 0.1 Hz. Electrodes: (a) Nafion/Hb/CILE, (b) Nafion/TiO_2–Hb/CILE, (c) Nafion/GR–Hb/CILE and (d) Nafion/GR–TiO_2–Hb/CILE.

CILE. The results indicated the conductivity of the composite film was enhanced due to the presence of TiO_2 nanorods or GR nanosheets. The Ret value of Nafion/GR–TiO_2–Hb/CILE was further decreased to 17.7 Ω (curve d), indicating the synergistic effects of GR and TiO_2 nanorods in the composite film resulted in the good conductivity with the decrease of the impedance.

3.4. Direct electrochemistry of Nafion/GR–TiO_2–Hb/CILE

Fig. 4 shows cyclic voltammograms of different electrodes in pH 3.0 PBS at a scan rate of 100 mV s^{-1}. No obvious redox peaks appeared on Nafion/GR–TiO_2/CILE (curve a), indicating no electroactive substances present on the electrode. Cyclic voltammograms of Nafion/Hb/CILE exhibited a pair of small and unsymmetric redox peaks (curve b), indicated that only few Hb molecules closest to the electrode surface could exchange electrons with slow rate. While on Nafion/TiO_2–Hb/CILE (curve c) and Nafion/GR–Hb/CILE (curve d) the electrochemical responses of Hb were enhanced with the increase of the redox peak currents, indicating that the addition of TiO_2 nanorods or GR on the electrode surface was benefit to improve the electron transfer rate of Hb with underlying electrode. Also the redox peak currents were bigger on GR based electrode than that of TiO_2 nanorods modified electrode, indicating the higher conductivity of GR than TiO_2 nanorods. However, on Nafion/GR–TiO_2–Hb/CILE (curve e) a couple of well-defined quasi-reversible redox peaks appeared and the responses were bigger than that of Nafion/GR–Hb/CILE or Nafion/TiO_2–Hb/CILE, indicating that GR–TiO_2 nanocomposite was benefit for the electron transfer of Hb. GR exhibit high

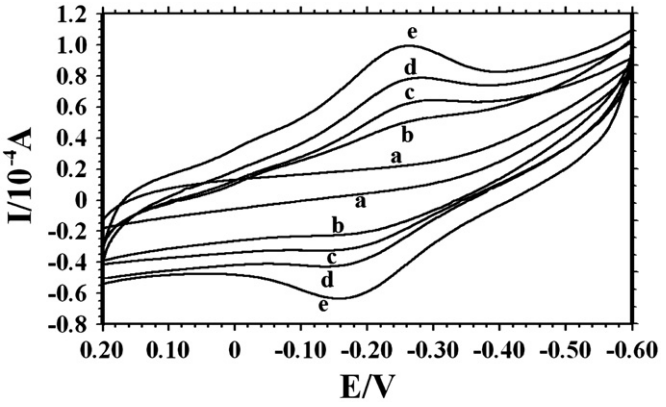

Fig. 4. Cyclic voltammograms of (a) Nafion/GR–TiO_2/CILE, (b) Nafion/Hb/CILE, (c) Nafion/TiO_2–Hb/CILE, (d) Nafion/GR–Hb/CILE and (e) Nafion/GR–TiO_2–Hb/CILE in pH 3.0 PBS with the scan rate as 100 mV s^{-1}.

conductivity with big porous structure and TiO_2 nanorods are biocompatible semiconductor with high surface area. So the GR–TiO_2 nanocomposite is benefit for the Hb immobilization. The anodic peak potential (Epa) of −0.163 V and the cathodic peak potential (Epc) of −0.269 V were recorded, which was corresponded to the reduction and oxidation of the electroactive center of Hb. The formal peak potential ($E^{0'}$), which is taken as the average of the anodic and cathodic peak potential, was estimated to be −0.216 V (vs. SCE), and it was the typical value of the active center of Hb Fe(III)/Fe(II) redox couple. The results can be

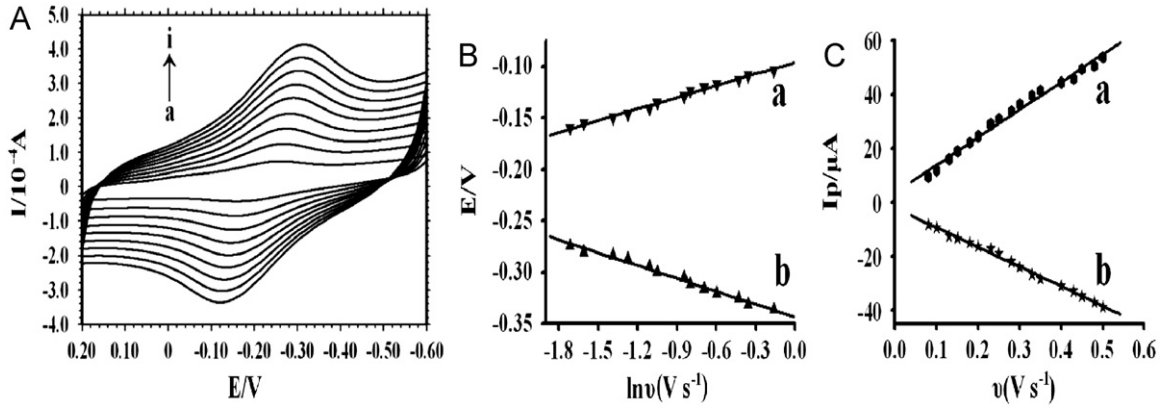

Fig. 5. (A) Influence of scan rate on electrochemical responses of Nafion/GR–TiO_2–Hb/CILE in pH 3.0 PBS with scan rates from (a) to (i) as 100, 200, 300, 400, 500, 600, 700, 800 and 900 mV s^{-1}, respectively. (B) Linear relationship of the peak potential Epa (a) and Epc (b) versus lnυ. (C) Linear relationship of cathodic (a) and anodic (b) peak current (Ip) versus scan rate (υ).

attributed to large surface-to-volume ratio, high conductivity and good biocompatibility of GR–TiO_2 nanocomposite that led to enhance the enzyme absorption and provide a suitable microenvironment for protein to transfer electrons with underlying electrode.

The influence of scan rate (υ) on the electrochemical response of the modified electrode was further investigated. As shown in Fig. 5A, cyclic voltammograms of Nafion/GR–TiO_2–Hb/CILE displayed a pair of well-defined quasi-reversible redox peaks at different scan rates with almost equal height of peak currents. With the increase of scan rate the redox peak currents varied linearly with scan rate in the range from 0.1 to 0.9 V s^{-1}. Two well-defined straight lines were got with the equations as Ipc(μA)=102.42 υ (V s^{-1})−10.32 (n=17, γ=0.993) and Ipa(μA)=−72.41 υ (V s^{-1})−2.1 (n=17, γ=0.998), respectively (as shown in Fig. 5B). The results manifested a typical surface-controlled electrochemical behavior. The surface coverage (Γ^*) can be estimated from integration of the reduction or oxidation peak of cyclic voltammograms with the equation ($\Gamma^*=Q/nAF$), where Q is the charge involved in the reaction, n is the number of electrons transferred, F is the Faraday constant, and A is the geometric area of electrode. By integration of the reduction peak currents the surface coverage (Γ^*) of electroactive Hb was calculated as 1.1×10^{-9} mol cm^{-2}, which was much larger than that of monolayer coverage (1.89×10^{-11} mol cm^{-2}) (Wang et al., 2005). While the total amounts of Hb cast on the electrode surface was calculated as 1.27×10^{-8} mol cm^{-2}, so the fraction of electroactive proteins among the total proteins on CILE surface was 8.7%. The results suggested that multilayers of Hb in the composite film close to the electrode with suitable orientation could exchange electron with electrode. With the increase of scan rate the redox peak potentials were also shifted gradually. As shown in Fig. 5C, the relationships of Ep with lnυ were constructed with two well-defined straight lines got as Epa (V)=0.038 lnυ (V/s)−0.09 (n=13, Γ=0.995) and Epc (V)=−0.042 lnυ (V/s)−0.34 (n=13, Γ=0.993). According to the Laviron's equations (Laviron, 1979), the values of the electron transfer coefficient (α) and the heterogeneous electron transfer rate constant (k_s) were estimated as 0.48 and 0.65 s^{-1}, respectively.

In most cases the redox behavior of protein is significantly dependent on the solution pH. So the influence of buffer pH on cyclic voltammograms of Nafion/GR–TiO_2–Hb/CILE was investigated in 0.1 mmol L^{-1} PBS. Nearly reversible voltammograms with stable and well-defined redox peaks were observed and the maximum redox peak current was occurred at pH 3.0, which was selected for the electrochemical investigation. Furthermore, negative shifts in both anodic and cathodic peak potentials were

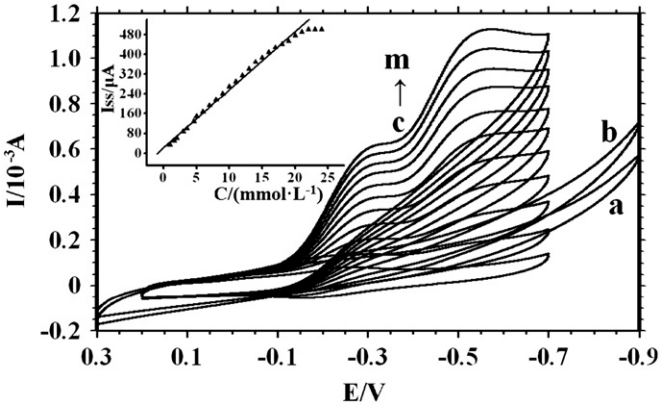

Fig. 6. Cyclic voltammograms of Nafion/GR–TiO_2/CILE with (a) 3.0, (b) 6.0 mmol L^{-1} TCA and Nafion/GR–TiO_2–Hb/CILE with 0, 2.0, 4.0, 6.0, 8.0, 10.0, 12.0, 14.0, 16.0, 19.0 and 22.0 mmol L^{-1} TCA (curves c–m) in 0.1 mol L^{-1} pH 3.0 PBS at the scan rate of 100 mV s^{-1} (inset was the linear relationship of catalytic peak currents and TCA concentration).

observed with increasing pH value from 1.5 to 6.0. The formal peak potential ($E^{0'}$) had a linear relationship with the buffer pH and the regression equation was calculated as $E^{0'}$(mV)=54.72−41.57 pH (n=5, Γ=0.987). The slope of −41.57 mV pH^{-1} was smaller than the theoretical value of −59.0 mV pH^{-1} for a one-electron–one-proton reaction between the electrode and each of the four heme Fe(III) of Hb. The reason might be the influence of the protonation states of transligands to the heme iron and amino acids around the heme or the protonation of the water molecule coordinated to the central iron. However, it also could indicate that a single protonation accompany with one electron transfer of Hb Fe(III) to electrode with the equation as: Hb Fe(III)+H^++e^-→Hb Fe(II).

3.5. Biocatalytic activity of Hb modified electrode

It is well-known that the redox proteins usually have good electrocatalytic activity towards TCA, which is an important target in the fields such as biochemistry and environmental analysis. Nafion/GR–TiO_2–Hb/CILE showed good electrocatalytic ability to TCA with the typical cyclic voltammograms as shown in Fig. 6. When TCA was added to pH 3.0 buffer, a great increase of the reduction peak was observed at −0.317 V with the simultaneously disappearance of the oxidation peak (curves c–m). However, no direct reduction peak was observed at Nafion/GR–TiO_2/CILE in the presence of TCA (curves a and b). The results can be

attributed to the electrocatalytic reduction of Hb in the modified electrode for TCA. With the further increase of the TCA concentration another new reduction peak appeared at −0.566 V. The peak could be attributed to the formation of a highly reduced form of Hb, which might dechlorinate di- and mono-chloroacetic acid after the dechlorination of TCA with Hb Fe(II) (Fan et al., 2000). Thus, the electrocatalytic reaction may be deduced via the following equations, which involved the reduction of Hb Fe(III) to Hb Fe(II), the reduction of TCA with Hb Fe(II), the reduction of Hb Fe(II) to Hb Fe(I), the reduction of di- and mono-chloroacetic acid with Hb Fe(II) and the reoxidation of Hb Fe(I).

$$\text{Hb Fe(III)} + e \rightarrow \text{Hb Fe(II)} \quad (1)$$

$$2\text{Hb Fe(II)} + Cl_3CCOOH + H^+ \rightarrow 2\text{Hb Fe(III)} + Cl_2CHCOOH + Cl^- \quad (2)$$

$$\text{Hb Fe(II)} + e \rightarrow \text{Hb Fe(I)} \quad (3)$$

$$2\text{Hb Fe(I)} + Cl_2CHCOOH + H^+ \rightarrow 2\text{Hb Fe(II)} + ClCH_2COOH + Cl^- \quad (4)$$

$$2\text{Hb Fe(I)} + ClCH_2COOH + H^+ \rightarrow 2\text{Hb Fe(II)} + CH_3COOH + Cl^- \quad (5)$$

The catalytic reduction peak current had a good linear relationship with TCA concentration in the range from 0.6 to 21.0 mmol L^{-1} with the regression equation as Ipc (μA)=23.49 C (mmol L^{-1})+21.40 (n=23, Γ=0.997) and the detection limit as 0.22 mmol L^{-1} (3σ). When the TCA concentration was more than 21.0 mmol L^{-1}, the current value reached a saturation limit, which indicated the Michaelis–Menten kinetic for the electrocatalytic reaction of TCA. The apparent Michaelis–Menten constant (K_M^{app}) could be calculated from the electrochemical version of the Lineweaver–Burk equation: $1/I_{ss}=(1/I_{max})(1+K_M^{app}/C)$, where I_{ss} is the steady current after the addition of substrate, C is the bulk concentration of the substrate, and I_{max} is the maximum current measured under saturated substrate condition (Kamin and Wilson, 1980). Then the K_M^{app} value was calculated to be 3.3 mmol L^{-1}, which was smaller than that of some previous reported values such as 5.13 mmol L^{-1} (Sun et al., 2009a) and 47.0 mmol L^{-1} (Wang et al., 2005). The lower value of K_M^{app} indicated that Hb immobilized on Nafion/GR–TiO_2/CILE retained its bioactivity and had a high biological affinity to TCA.

3.6. Stability and reproducibility of Nafion/GR–TiO_2–Hb/CILE

The stability of Nafion/GR–TiO_2–Hb/CILE was further studied by electrochemical method. After the modified electrode was stored in a refrigerator at 4 °C for two weeks, 4.2% decrease of peak current appeared. After a 30-day storage, Nafion/GR–TiO_2–Hb/CILE still retained 90.5% of its initial current response, which indicated that this electrode had good stability (the results are shown in Fig. S1). When a 10.0 mmol L^{-1} TCA solution was determined with 10 modified electrodes made independently, cyclic voltammograms were recorded with the relative standard deviations (RSD) of the current were calculated as 4.38% (to avoid confusion, 5 cyclic voltammetric curves are shown in Fig. S2). These results indicated an efficient and reproducible immobilization process of Hb in GR–TiO_2 nanocomposite film.

4. Conclusions

On Nafion/GR–TiO_2–Hb/CILE a pair of well-defined redox peaks appeared on cyclic voltammograms, which was corresponded to the direct electrochemistry of Hb with a one-proton one-electron transfer. By combining the advantages of GR and TiO_2 nanorods, GR–TiO_2 nanocomposite exhibited high conductivity with big surface area and good biocompatibility, which facilitated the direct electron exchange between Hb and electrode. The immobilized Hb retained its native structure in GR–TiO_2 nanocomposite with good electrocatalytic ability. Based on GR–TiO_2 nanocomposite the new third-generation electrochemical biosensor was fabricated for TCA detection with high sensitivity, wide linear range, low detection limit, long-term stability and good reproducibility. So the GR–TiO_2–Hb films may have a potential application in constructing biosensors based on mediator-free electrochemistry of the enzymes.

Acknowledgments

We acknowledge the financial support of the National Natural Science Foundation of China (No. 21075071) and the Foundation of Hainan Normal University.

Appendix A. Supporting information

Supplementary data associated with this article can be found in the online version at http://dx.doi.org/10.1016/j.bios.2012.10.034.

References

Armstrong, F.A., Hill, H.A.O., Walton, N., 1988. Accounts of Chemical Research 21, 407–413.
Armstrong, F.A., Wilson, G.S., 2000. Electrochimica Acta 45, 2623–2645.
Bao, S.J., Li, C.M., Zang, J.F., Cui, X.Q., Qiao, Y., Guo, J., 2008. Advanced Functional Materials 18, 591–599.
Byler, D.M., Susi, H., 1986. Biopolymers 25, 469–487.
Chen, D., Tang, L.H., Li, J.H., 2010. Chemical Society Reviews 39, 3157–3180.
Chen, H., Müller, M.B., Gilmore, K.J., Wallace, G.G., Li, D., 2008. Advanced Materials 20, 3557–3561.
Deng, K.Q., Zhou, J.H., Li, X.F., 2013. Colloid Surface B 101, 183–188.
Fan, C.H., Zhuang, Y., Li, G.X., Zhu, J.Q., Zhu, D.X., 2000. Electroanalysis 12, 1156–1158.
Gan, T., Hu, S.S., 2011. Microchimica Acta 175, 1–19.
Geim, A.K., Novoselov, K.S., 2007. Natural Materials 6, 183–191.
Guo, S.J., Dong, S.J., 2011. Chemical Society Reviews 40, 2644–2672.
Hummers, W.S., Offeman, R.E., 1958. Journal of the American Chemical Society 80, 1339–1399.
Jang, H.D., Kim, S.K., Chang, H., Roh, K., Choi, J., Huang, J.X., 2012. Biosensors & Bioelectronics 38, 184–188.
Kamin, R.A., Wilson, G.S., 1980. Analytical Chemistry 52, 1198–1205.
Kauppinen, J.K., Moffat, D.J., Mantsch, H.H., Cameron, D.G., 1981. Applied Spectroscopy 35, 271–276.
Laviron, E., 1979. Journal of Electroanalytical Chemistry 101, 19–28.
Leger, C., Elloitt, S.J., Hoke, K.R., Jeuken, L.J.C., Jones, A.K., Armstrong, F.A., 2003. Biochemistry 42, 8653–8662.
Li, J., Guo, S.J., Zhai, Y.M., Wang, E.K., 2009. Electrochemistry Communications 11, 1085–1088.
Li, Q.W., Luo, G., Feng, J., 2001. Electroanalysis 13, 359–363.
Lu, X.B., Zou, G.F., Li, J.H., 2007. Journal of Materials Chemistry 17, 1427–1432.
Nadzhafova, O.Y., Zaitsev, V.N., Drozdova, M.V., Vaze, A., Rusling, J.F., 2004. Electrochemistry Communications 6, 205–209.
Opallo, M., Lesniewski, A., 2011. Journal of Electroanalytical Chemistry 656, 2–16.
Rusling, J.F., Kumosinski, T.F., 1992. Instruments & Computers 10, 139–145.
Rusling, J.F., Nassar, A.F., 1993. Journal of the American Chemical Society 115, 11891–11897.
Shangguan, X.D., Zhang, H.F., Zheng, J.B., 2008. Analytical and Bioanalytical Chemistry 391, 1049–1055.
Shao, Y.Y., Wang, J., Wu, H., Liu, J., Aksay, I.A., Lin, Y.H., 2010. Electroanalysis 22, 1027–1036.
Singh, V., Joung, D., Zhai, L., Das, S., Khondaker, S.I., Seal, S., 2011. Progress in Materials Science 56, 1178–1271.
Sun, J.Y., Huang, K.J., Zhao, S.F., Fan, Y., Wu, Z.W., 2011. Bioelectrochemistry 82, 125–130.
Sun, W., Li, Y.Z., Duan, Y.Y., Jiao, K., 2008. Biosensors & Bioelectronics 24, 988–993.
Sun, W., Li, X.Q., Wang, Y., Zhao, R.J., Jiao, K., 2009a. Electrochimica Acta 54, 4141–4148.
Sun, W., Li, X.Q., Liu, S.F., Jiao, K., 2009b. Bulletin of the Korean Chemical Society 30, 582–5889.
Topoglidis, E., Campbell, C.J., Cass, A.E.G., Durrant, J.R., 2001. Langmuir 17, 7899–7905.
Topoglidis, E., Lutz, T., Willis, R.L., Barnett, C.J., Cass, A.E.G., Durrant, J.R., 2000. Faraday Discussions 116, 35–46.
Wang, D.H., Choi, D.W., Li, J., Yang, Z.G., Nie, Z.M., Kou, R., Hu, D.H., Wang, C.M., Saraf, L.V., Zhang, J.G., Aksay, I.A., Liu, J., 2009a. ACS Nano 3, 907–914.

Wang, S.F., Chen, T., Zhang, Z.L., Shen, X.C., Lu, Z.X., Pang, D.W., Wong, K.Y., 2005. Langmuir 21, 9260–9266.
Wang, Y., Li, Y.M., Tang, L.H., Lu, J., Li, J.H., 2009b. Electrochemistry Communications 11, 889–892.
Wu, D., Liu, J., Zhao, X.N., Li, A.D., Chen, Y.F., Ming, N.B., 2006. Chemistry of Materials 18, 547–553.
Wu, J.F., Xu, M.Q., Zhao, G.C., 2010. Electrochemistry Communications 12, 175–177.
Xu, H.F., Dai, H., Chen, G.N., 2010. Talanta 81, 334–338.
Zhang, H., Lv, X.J., Li, Y.M., Wang, Y., Li, J.H., 2010. ACS Nano 4, 380–386.
Zhang, Y., He, P.L., Hu, N.F., 2004. Electrochimica Acta 49, 1981–1988.
Zhang, Y., Zheng, J.B., 2007. Electrochimica Acta 52, 7210–7216.
Zheng, W., Zheng, Y.F., Jin, K.W., Wang, N., 2008. Talanta 74, 1414–1419.
Zhu, Y.C., Cheng, G.J., Dong, S.J., 2002. Biophysical Chemistry 97, 129–138.
Zhu, Y.W., Murali, S., Cai, W.W., Li, X.S., Suk, J.W., Potts, J.R., Ruoff, R.S., 2010. Advanced Materials 22, 3906–3924.
Zou, F., Yu, Y., Cao, N., Wu, L.Z., Zhi, J.F., 2011. Scripta Materialia 64, 621–624.